Supporting Information

McCullough *et al.* 10.1073/pnas.0801567105

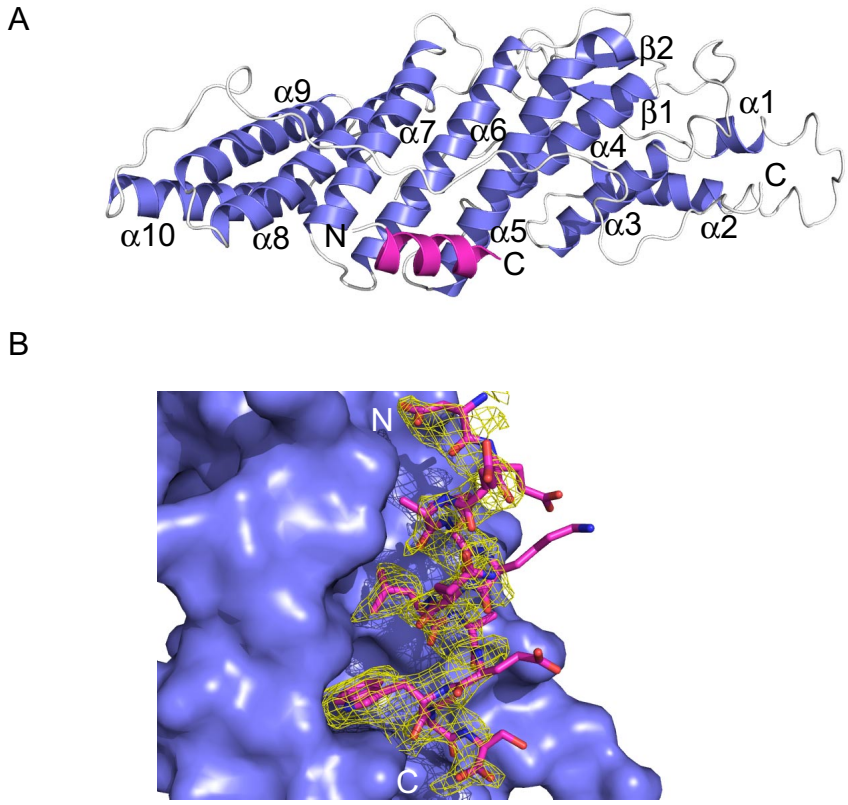

Fig. S1. ALIX$_{Bro1}$ in complex with the C-terminal CHMP4A helix. (*A*) Ribbon diagram showing the complex between ALIX$_{Bro1}$ and the C-terminal helix from CHMP4A (purple). This figure is oriented so that the CHMP4A helix in Fig. 1 *Lower* is rotated ≈90° toward the viewer. (*B*) CHMP4A is represented in sticks against a solid ALIX surface, with the Fo-Fc peptide omit map contoured at 2 × rmsd and displayed over the peptide. To generate the peptide omit map, the peptide was deleted from the model, random shifts (0.3 Å in *x*, *y*, *x*) were applied throughout and the model rerefined without the peptide in REFMAC. The orientation is the same as in Fig. 3.

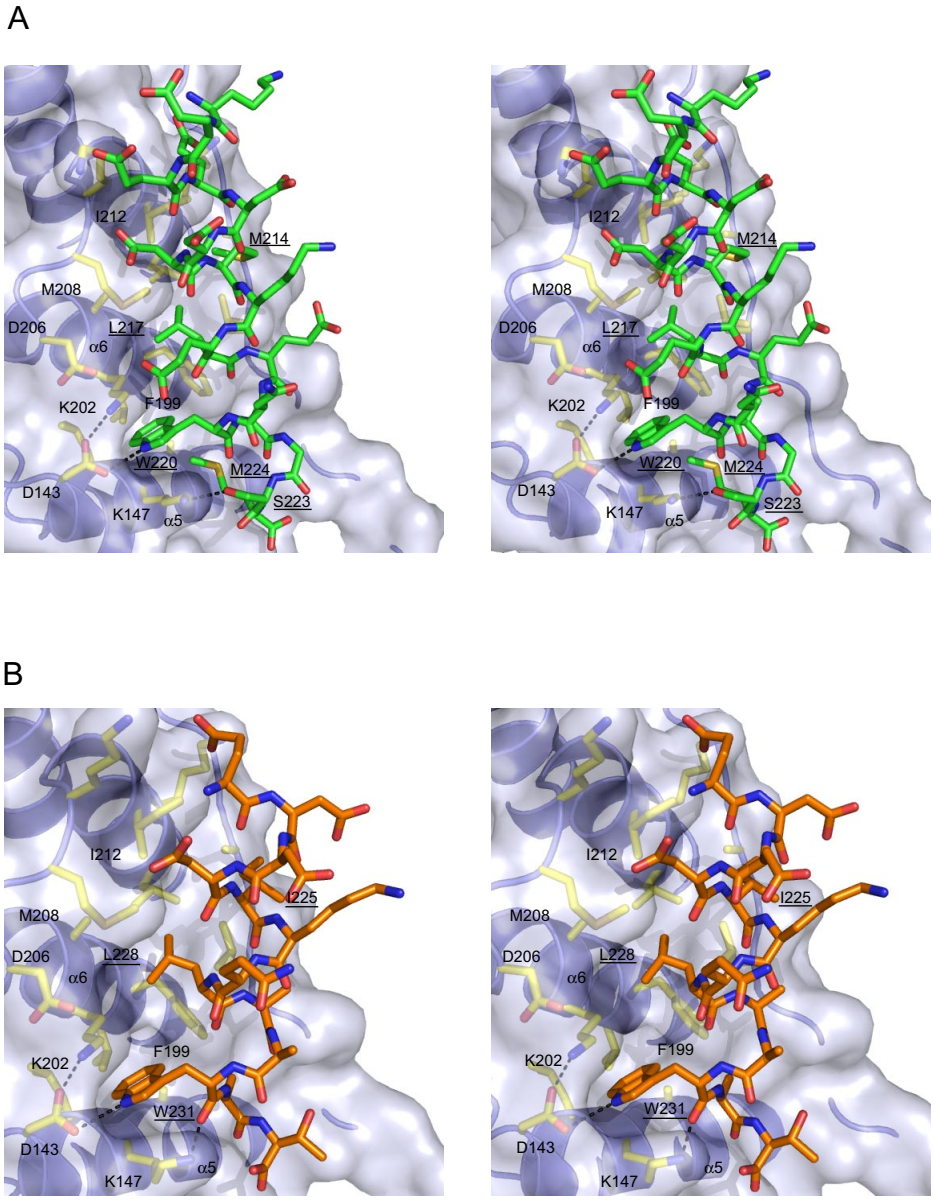

Fig. S2. Stereoviews of $ALIX_{Bro1}$-CHMP4B and $ALIX_{Bro1}$-CHMP4C interfaces. (*A*) $ALIX_{Bro1}$-CHMP4B. (*B*) $ALIX_{Bro1}$-CHMP4C. Views and designations are the same as in Fig. 3*A*, except that CHMP4B is shown in green and CHMP4C is shown in orange.

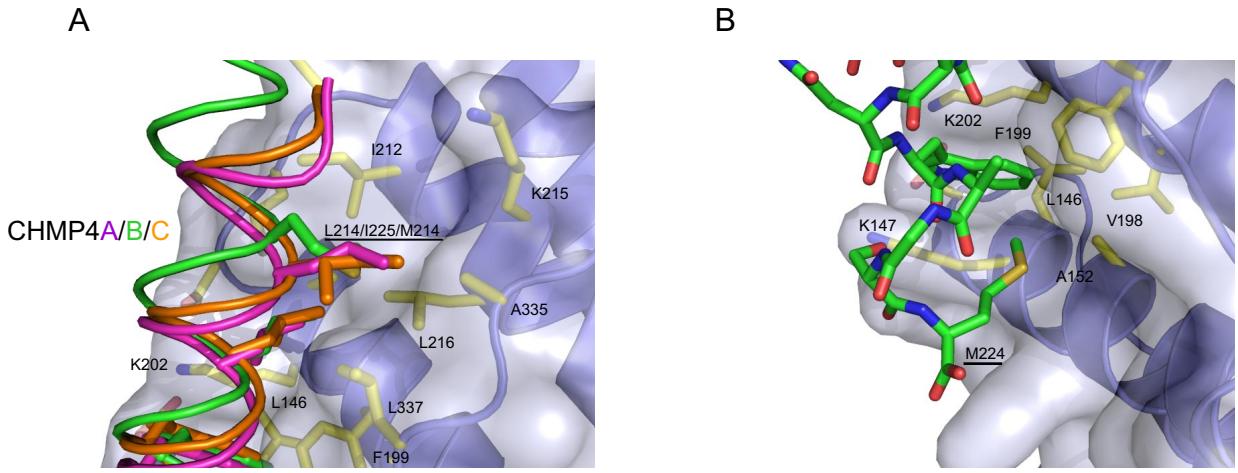

Fig. S3. Comparative analyses of the $ALIX_{Bro1}$-CHMP4B interface. (*A*) Overlay of $ALIX_{Bro1}$-bound CHMP4A-C helices illustrating how hydrophobic residues at the N-terminal ends of the helices can make nearly equivalent contacts despite displacement of the CHMP4B helix (green). (*B*) Expanded view of the CHMP4B C terminus, highlighting the unique $ALIX_{Bro1}$ contacts made by the C-terminal Met-224 residue.

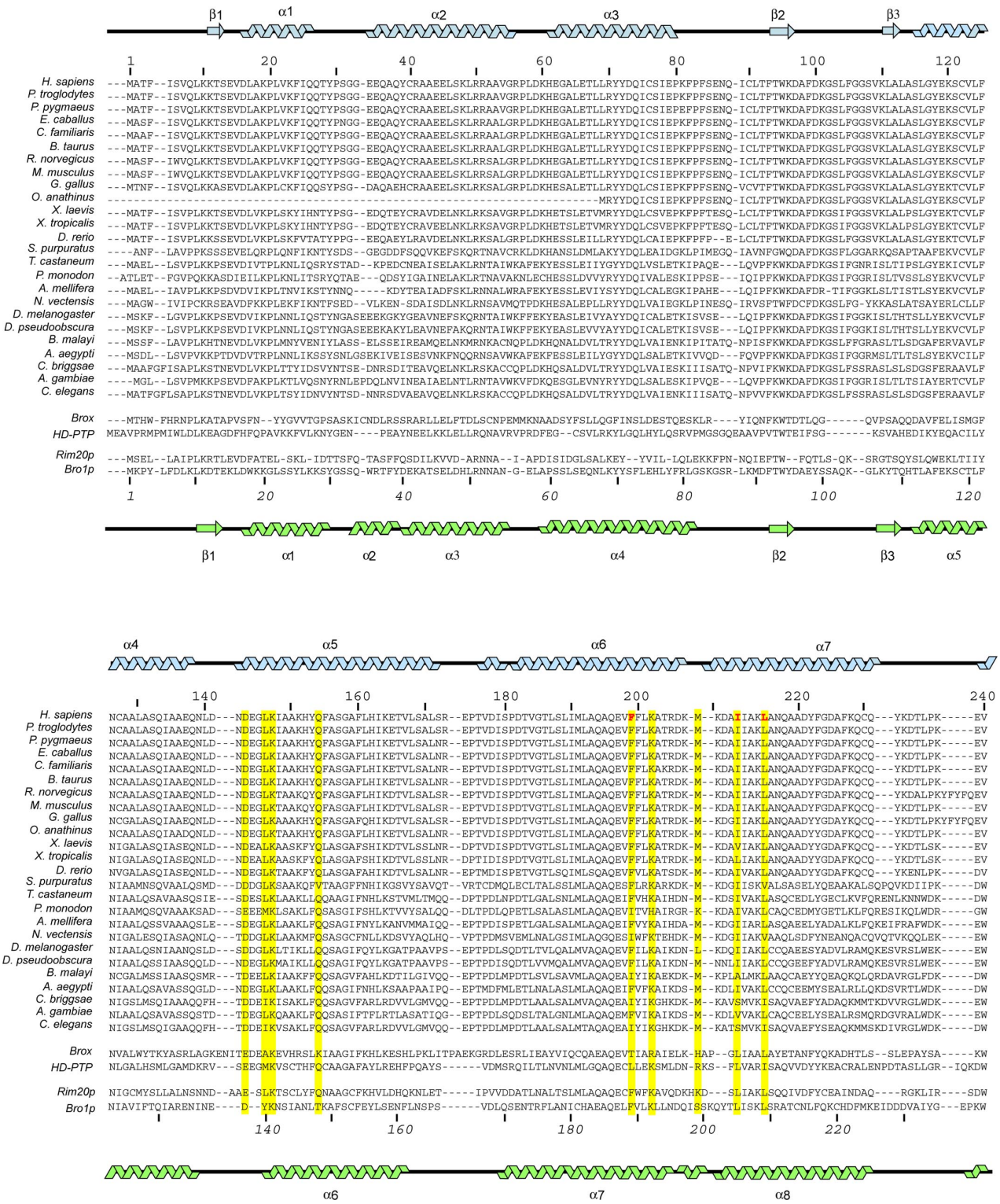

Fig. S4. (Continued on next page.)

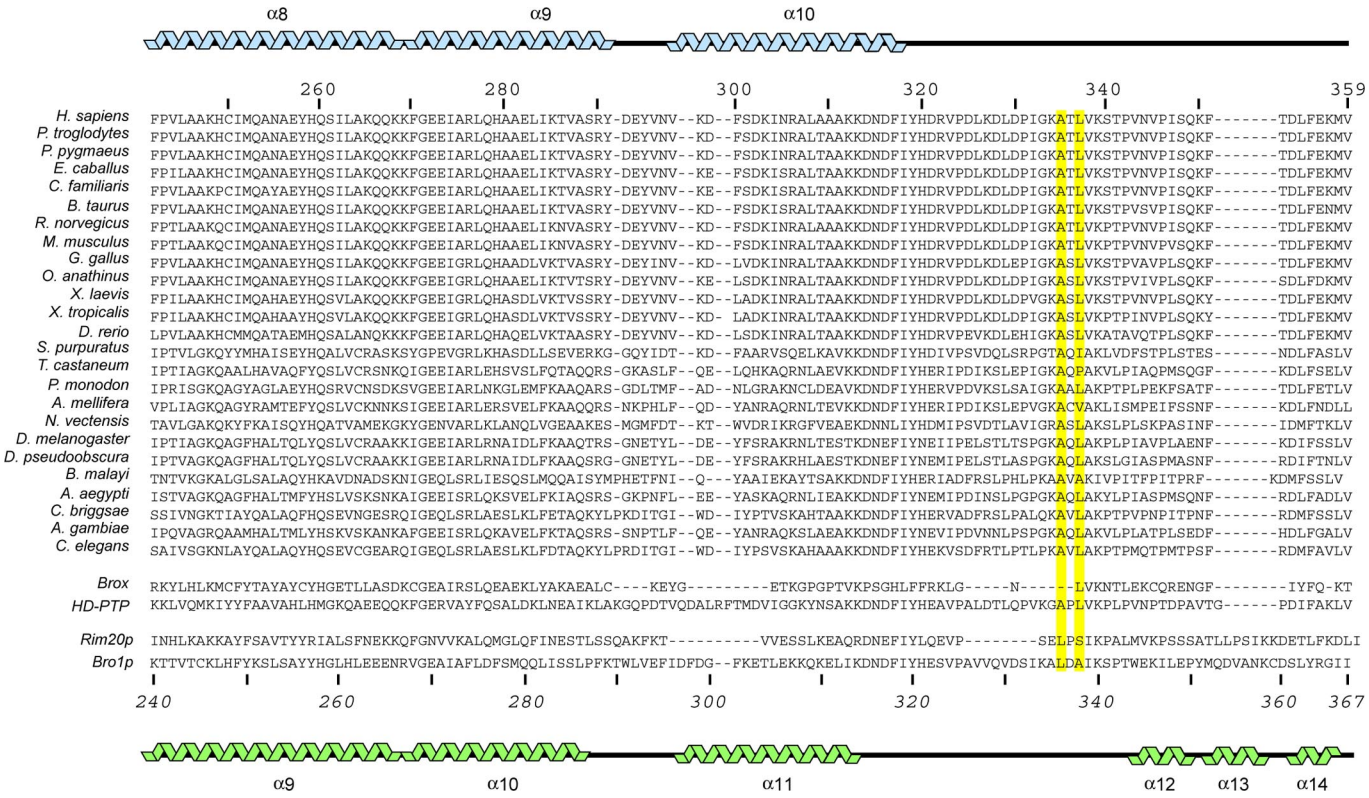

Fig. S4 (Continued). Sequence alignments and secondary structures of Bro1 domains. Secondary structures of the Bro1 domain of ALIX (*Upper*) and Bro1p (*Lower*) (PDB entry 1zb1) are shown together with aligned primary sequences of $ALIX_{Bro1}$ domains from 25 representative metazoan species (top sequence block), Bro1 domains from the human Brox and HD-PTP proteins (middle sequence block), and Bro1 domains from the yeast Rim20p and Bro1p proteins (bottom sequence block). $ALIX_{Bro1}$ and Bro1p were aligned by least squares overlap of the two structures, and other sequence alignments were performed by using the ClustalW server http://npsa-pbil.ibcp.fr/NPSA/npsa_clustalw.html [Combet C, Blanchet C, Geourjon C, Deléage (2000) NPS@: Network protein sequence analysis. *Trends Biochem Sci* 25:147–150]. Residues highlighted in yellow make contacts with CHMP4A in the ALIXBro1-$CHMP4A_{205–222}$ structure and residues italicized in bold and red block ALIX binding and HIV-1 budding when mutated to Asp.

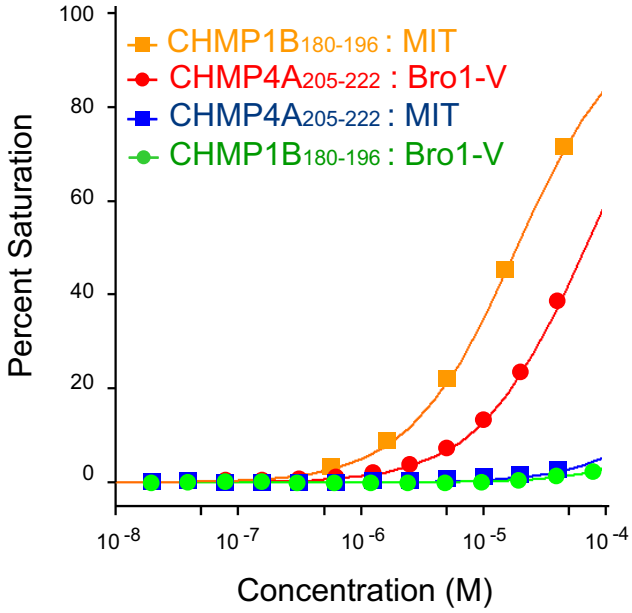

Fig. S5. Selectivity of the CHMP4A and CHMP1B recognition helices for $ALIX_{Bro1\text{-}V}$ and Vps4A MIT. Biosensor isotherms showing $ALIX_{Bro1\text{-}V}$ and VPS4A MIT domain binding to immobilized GST-$CHMP4A_{205\text{-}222}$ and GST-$CHMP1B_{180\text{-}196}$. Estimated dissociation constants for $ALIX_{Bro1\text{-}V}$ interactions were: GST-$CHMP4A_{205\text{-}222}$, 44 ± 6 μM, GST-$CHMP1B_{180\text{-}196}$, > 1 mM. Estimated dissociation constants for VPS4A MIT domain interactions were: GST-$CHMP4A_{205\text{-}222}$, > 1 mM, GST-$CHMP1B_{180\text{-}196}$, 18.5 ± 0.6 μM (dissociation constant and error were estimated from a statistical fit of a single binding isotherm derived from duplicate measurements at six different Vps4A MIT domain concentrations over a range of 0–140 μM). Binding to a control GST surface was negligible in all cases (data not shown).

Table S1. Data collection and refinement statistics for $ALIX_{Bro1}$–CHMP4 complexes

Statistic	CHMP4A	CHMP4B	CHMP4C
Data collection			
Space group	C2	C2	C2
Cell dimensions			
a, *b*, *c*, Å	120.7, 62.7, 76.1	120.5, 62.6, 76.1	120.9, 62.4, 76.4
b, deg.	122.1	121.5	121.6
Resolution, Å	50.0–2.15 (2.23–2.15)	50.0–2.1 (2.18–2.10)	50.0–2.02 (2.09–2.02)
R_{sym}	0.063 (0.334)	0.067 (0.413)	0.066 (0.596)
$I/\sigma(I)$	19 (1.8)	14 (1.7)	9 (1.5)
Completeness, %	94.9 (75.1)	92.3 (67.6)	95.5 (81.0)
Redundancy	9.5 (3.8)	7.2 (4.6)	6.6 (4.4)
Refinement			
Resolution, Å	50.0–2.15 (2.21–2.15)	50.0–2.10 (2.154–2.10)	50.0–2.02 (2.07–2.02)
Reflections, no.	25,024	26,458	30,381
R_{work}	0.214 (0.305)	0.228 (0.326)	0.243 (0.333)
R_{free}	0.284 (0.344)	0.290 (0.386)	0.291 (0.411)
Number of atoms			
Protein	2911	2953	2905
Ligand/ion	6	6	6
Water	127	90	56
$\langle B \rangle$-factors			
Protein	33.2	35.3	34.0
Ligand/ion	82.5	78.9	85.8
Water	49.9	55.0	51.3
rmsd			
Bond lengths, Å	0.019	0.017	0.016
Bond angles, deg.	1.710	1.653	1.542
Ramachandran plot, %			
Most favored	89.7	88.0	90.6
Additionally allowed	9.7	10.8	8.6
Generously allowed	0.3 (Q27)	1.2 (K207,Q27,S31,C40)	0.3 (K207)
Disallowed	0.3 (Q88)	0.0	0.6 (Y29, E34)

Diffraction data from one crystal were used to determine each structure. This includes the CHMP4A complex, for which data were collected in two separate sweeps from different beamlines. Values in parentheses refer to the high-resolution shell.

Table S2. Thirty-four different CHMP4 protein sequences from 19 different metazoan species grouped together with the human CHMP4 isoform with which they show the greatest pair-wise identity throughout the entire protein

CHMP4 protein	Organism	NCBI protein accession no.	Overall identity to most homologous human CHMP4, %	C-terminal sequence
4A	*Homo sapiens*	Q9BY43	100	PKVDEDEEA**L**KQ**L**AE**W**VS
4A	*Pan troglodytes*	XP_001169270	99(A)	PKVDEDEEA**L**KQ**L**AE**W**VS
4A	*Canis familiaris*	XP_537387	91(A)	PEADEDEAA**L**KQ**L**AE**W**VS
4A	*Bos taurus*	AAI33472	91(A)	PKADEDEAE**L**KQ**L**AE**W**VS
4A	*Monodelphis domestica*	XP_001380207	81(A)	ASKTDEEKE**M**KQ**L**VD**W**VS
4B	*Homo sapiens*	NP_789782	100	KKKEEEDDD**M**KE**L**EN**W**AGSM
4B	*Mus musculus*	NP_083638	99(B)	KKKEEEDDD**M**KE**L**EN**W**AGSM
4B	*Macaca mulatta*	XP_001105255	99(B)	KKKEEEDDD**M**KE**L**EN**W**AGSM
4B	*familiaris*	XP_542966	97(B)	KKKEEEEDD**M**KE**L**EN**W**AGSM
4B	*Bos taurus*	AAI23448	97(B)	KKKEEEDED**M**KE**L**ET**W**AGTI
4B	*Rattus norvegicus*	XP_001073409	97(B)	KKKEEEDDD**M**KE**L**EN**W**AGSM
4B	*Monodelphis domestica*	XP_001381361	96(B)	KKKEEEDDD**M**KE**L**EN**W**AGSM
4B	*Ornithorhynchus anatinus*	XP_001518785	94(B)	KKKEEEDDD**M**KE**L**EN**W**AGSM
4B	*Equus caballus*	XP_001499057	94(B)	KKKEEEDDD**M**KE**L**EN**W**AGTI
4B	*Gallus gallus*	NP_001006286	91(B)	KKEEEEDDD**M**KE**L**EA**W**AGNM
4B	*Xenopus laevis*	Q5XGW6	87(B)	KKQEEDDDD**M**RE**L**EN**W**ATA
4B	*Xenopus tropicalis*	Q6GL11	87(B)	KKQEEDDDD**M**RE**L**EN**W**ATA
4B	*Danio rerio*	Q7ZVC4	86(B)	KKEEEDEDD**M**KD**L**EA**W**AAN
4B	*Nematostella vectensis*	XP_001639344	67(B)	AKKKTEDDD**L**AE**L**EA**W**AS
4B	*Ornithodoros moubata*	AAS59855	66(B)	SKAVMEDPD**M**IE**L**AQ**W**AS
4B	*Anopheles gambiae*	XP_315330	64(B)	AVAEEDDPD**M**KE**L**MS**W**AN
4B	*Caenorhabditis elegans*	AAA68771	61(B)	PRAKEADKD**L**ED**L**ES**W**AN
4B	*Drosophila melanogaster*	NP_610462	57(B)	AVEDDDDPD**M**KQ**L**LS**W**SN
4C	*Homo sapiens*	Q96CF2	100	QRAEEEDDD**I**KQ**L**AA**W**AT
4C	*Pan troglodytes*	XP_528179	99(C)	RRAEEEDDD**I**KQ**L**AA**W**AT
4C	*Macaca mulatta*	XP_001093735	98(C)	RRAEEEDDD**I**KQ**L**AA**W**AT
4C	*Canis familiaris*	XP_535115	88(C)	SKRTEEVDD**I**KQ**L**AA**W**AP
4C	*Bos taurus*	AAI13332	88(C)	RRTEGEDDD**I**QH**L**AA**W**AT
4C	*Monodelphis domestica*	XP_001367000	88(C)	SRRKEDEDD**I**KQ**L**AA**W**AS
4C	*Equus caballus*	XP_001489156	87(C)	RRAEEDDDD**I**KK**L**SA**W**AT
4C	*Mus musculus*	Q9D7F7	84(C)	SRRAEEDDD**F**KQ**L**AA**W**AT
4C	*Rattus norvegicus*	Q569C1	84(C)	SRRAEEDDD**F**KQ**L**AA**W**AT
4C	*Gallus gallus*	XP_418312	72(C)	RRRVEDEDD**M**KQ**L**AA**W**AS
4C	*Xenopus laevis*	Q6GNN8	69(C)	SKKVEDDDD**M**QM**L**AA**W**AT

Conserved hydrophobic, Leu, and Trp positions in the terminal recognition helix are in bold. For reference, pairwise identities between the three human CHMP4 isoforms are 62% (A vs. B), 52% (A vs. C), and 61% (B vs. C), whereas the nearest identity between a human CHMP4 protein and another human CHMP protein is 30% (CHMP4A vs. CHMP5). Note that our current nomenclature for CHMP4A (NCBI protein accession locus Q9BY43), CHMP4B (NP_789782), and CHMP4C (Q96CF2) matches the current NCBI database annotations (www.ncbi.nlm.nih.gov/sites/entrez) but that the designations of CHMP4A and CHMP4B are reversed from those used in several previous publications.